

Joint Data Collection and Sensor Positioning in Multi-UAV-Assisted Wireless Sensor Network

Mingyue Zhu, Zhiqing Wei, Chen Qiu, Wangjun Jiang, Huici Wu, and Zhiying Feng

Abstract—Due to the high mobility and easy deployment, unmanned aerial vehicles (UAVs) have attracted much attention in the field of wireless communication and positioning. To meet the challenges of lack of infrastructure coverage, uncertain sensor position and large amount of sensing data collection in wireless sensor network (WSN), this paper presents an efficient joint data collection and sensor positioning scheme for WSN supported by multiple UAVs. Specifically, a UAV is set as the main UAV to collect data, and other UAVs are used as auxiliary UAVs for sensor positioning using time difference of arrival (TDoA). A mixed-integer non-convex optimization problem with uncertain sensor position is established. The goal is to minimize the average positioning error of all sensors by jointly optimizing the UAV trajectories, sensor transmission schedule and positioning observation points (POPs). To solve this optimization model, the original problem is decomposed into two sub-problems based on the path discrete method. Firstly, the block coordinate descent (BCD) and successive convex approximation (SCA) techniques are applied to iteratively optimize the trajectory of the main UAV and the sensor transmission schedule, so as to maximize the minimum amount of data uploaded by the sensor. Then, based on the trajectory of the main UAV, a particle swarm optimization (PSO)-based algorithm is designed to optimize the POPs of UAVs. Finally, the spline curve is applied to generate the trajectories of auxiliary UAVs. The simulation results show that the proposed scheme can meet the requirements of data collection and has a good positioning performance.

Index Terms—Unmanned Aerial Vehicle, Wireless Sensor Network, Sensor Positioning, Data Collection, Time Difference of Arrival, Resource Allocation.

I. INTRODUCTION

Wireless sensor network (WSN) is an important component of the Internet of Things (IoT), which is composed of a large number of static or mobile sensors with sensing, computing and wireless communication capabilities. Due to the characteristics of wide coverage, low cost and remote monitoring, WSN is widely used in agriculture [1], industry [2], environmental monitoring [3], [4], intelligent transportation [5], etc., which is responsible for sensing, collecting, processing and transmitting the sensing information [6].

However, with the advancement and application of WSN, the amount of sensing data is also increasing significantly.

Mingyue Zhu, Zhiqing Wei, Wangjun Jiang and Zhiyong Feng are with School of Information and Communication Engineering, Beijing University of Posts and Telecommunications (BUPT), Beijing 100876, China. (e-mail: mingyue_zhu@bupt.edu.cn, weizhiqing@bupt.edu.cn, jiang-wangjun@bupt.edu.cn, fengzy@bupt.edu.cn).

Chen Qiu is with Peng Cheng Laboratory, Shenzhen, China. (e-mail: qiuch@pcl.ac.cn).

Huici Wu is with National Engineering Research Center of Mobile Network Technologies, Beijing University of Posts and Telecommunications (BUPT), Beijing, 100876, China, and also with Peng Cheng Laboratory, Shenzhen, China. (e-mail: dailywu@bupt.edu.cn).

However, data collection of sensors remains a challenge in the areas that lack infrastructure support, such as forests, oceans and islands. Besides, sensors are widely distributed and their positions are difficult to be acquired in advance [7]. Therefore, it is necessary to locate sensors for WSN, which will facilitate identifying where events occur [8], [9]. In addition, the location information of sensor could be applied in the optimization of data collection scheme, further improving the performance of WSN via the collaboration between data collection and sensor positioning. Hence, the data collection and sensor positioning are crucial for WSN.

With the development of UAV technology, UAV with strong coverage and mobility provides new opportunities for data collection of WSN [10], [11], [12]. In addition, the ability to be deployed quickly, move flexibly, and establish the line-of-sight (LoS) connection with high probability makes UAV-assisted positioning highly attractive [13]. The UAV equipped with Global Positioning System (GPS) and wireless communication modules can be used as mobile anchor nodes to estimate the positions of sensors by broadcasting or receiving positioning signals [14]. Therefore, the joint data collection and sensor positioning using UAVs is promising in WSN.

A. Related Work

Traditionally, sensor positioning and data collection in WSN are addressed separately. For example, the data collection schemes are designed assuming that the location information of sensors is known [15], [16]. And the positioning methods of sensors are addressed alone [17].

1) *UAV-assisted data collection schemes*: In terms of UAV-assisted data collection when the location information of sensors is known, Liu *et al.* [18] applied the age of information (AoI) to model the information timeliness of data collection. Then, a method of selecting data collection points is proposed. Dynamic programming and genetic algorithm (GA) are applied to optimize the trajectory of UAV to minimize the maximum and average AoI, respectively. To reduce the energy consumption of WSN, Chen *et al.* [19] proposed a data collection scheme considering network heterogeneity. A method jointly optimizing the operation mode of sensors, energy consumption threshold and cluster head selection is proposed to extend the network lifetime. Chen *et al.* [20] studied the WSN with periodic data collection requirements. To minimize the flight trajectory of UAV and energy consumption of sensors, a two-stage task planning strategy is proposed, which adopts ant colony optimization (ACO) algorithm and data-aware strategy to optimize the trajectory of UAV and the location of data collection points.

In terms of UAV-assisted data collection without the location information of sensors, Wang *et al.* [21] proposed a heuristic algorithm to optimize the trajectory of UAV to minimize the completion time of data transmission considering the constraints of UAV flight speed, acceleration, communication distance and communication throughput. In [22], Yin *et al.* optimized the trajectory of UAV in the scenario of UAV-assisted cellular network to improve the uplink sum rate. With the information of the position, transmit power and channel state information of the ground user unknown, a deterministic policy gradient algorithm is proposed to enable the UAV to track the ground user.

2) *UAV-assisted sensor positioning schemes*: The sensor positioning schemes in WSN include received signal strength (RSS), time of arrival (ToA) and time difference of arrival (TDoA) methods, which have high positioning accuracy and reliability. Among them, RSS-based positioning methods are widely applied in sensor positioning because of easy deployment and low cost [23], [24], [25]. In [23], a static sensor positioning scheme based on RSS is proposed, which takes into account the variation of path loss factor and shadow factor due to UAV height, and explores the impact of the number of UAVs and flight height on positioning error. On this basis, Sallouha *et al.* [24] assumed that the UAV follows a predetermined circular trajectory and collects RSS measurements at specific points. Then, the positioning accuracy is improved with limited energy by optimizing the UAV trajectory parameters, including UAV height, hover time, flight distance and the number of positioning points. Zou *et al.* [25] localized mobile nodes with multiple UAVs considering the time-varying of path-loss factor. The method combining least-mean-square (LMS) and iterative Newton gradient algorithm is proposed. Since the RSS-based positioning schemes have low positioning accuracy, Yuan *et al.* [26] proposed a UAV path planning and ToA positioning scheme in the Non-LoS (NLoS) environment. However, ToA is time-dependent and requires a high-accurate time synchronization. In contrast, TDoA does not require the time synchronization between UAV and sensor, which is more practical compared with ToA scheme.

Overall, the above independent research on data collection and sensor positioning has some deficiencies. In the scenario of UAV-assisted data collection, some studies assume that the location information of sensors is known without the design of positioning scheme, which is not practical. Besides, if data collection and sensor positioning are executed separately, additional communication and energy resources will be consumed. Hence, the joint data collection and sensor positioning scheme is required.

3) *UAV-assisted joint data collection and sensor positioning schemes*: Wang *et al.* [27] applied a UAV to assist ground base stations (BSs) in data collection and positioning of devices. The device transmits data to the UAV or BS based on the transmission rate at each time slot. And the UAV only provide positioning services at positions with the best positioning performance on the trajectory. To minimize the maximum energy consumption of all devices and ensure the required positioning accuracy, a differential evolution (DE) is proposed to jointly optimize the UAV trajectory and device transmis-

sion schedule. However, the proposed solution requires the assistance of BSs in data collection and positioning, which cannot be applied to areas lacking infrastructure coverage. In addition, the population initialization of DE is a difficulty due to a large number of variables. In [28], Zhu *et al.* applied a UAV to preliminarily realize joint sensor positioning and data collection through RSS technology and hovering based on the designed trajectory. Notwithstanding, the positioning accuracy is low due to RSS technology and the energy consumption of UAV is high due to the traversal trajectory.

B. Contributions and Organization

In view of the above limitations, we propose a joint data collection and sensor positioning scheme using multiple UAVs in WSN. A joint optimization framework is proposed to minimize the average positioning error of all sensors while satisfying the data collection requirements for sensors. The main contributions of this paper are summarized as follows.

- 1) The multiple UAVs are applied as the data collector and mobile anchor to provide new solutions for data collection and sensor positioning. One UAV acts as the main UAV that is responsible for collecting sensing data, while the other UAVs apply TDoA technology in sensor positioning. Considering the constraints of the flight energy consumption, flight speed, requirements for data collection and communication range, a mixed-integer non-convex optimization model is established. The optimization model is to optimize the UAV flight trajectory, sensor transmission schedule and positioning observation points (POPs) jointly to minimize the average positioning error of sensors, while ensuring the amount of data collection. In particular, the optimization model takes into account the uncertainty of sensor position, which is more practical.
- 2) The original problem is decomposed into two sub-problems, namely sub-problem 1: joint data collection and main UAV trajectory optimization, and sub-problem 2: joint sensor positioning and auxiliary UAV trajectory optimization. For sub-problem 1, an iterative algorithm for solving mixed non-convex problems is proposed using the block coordinate descent (BCD) and successive convex approximation (SCA) techniques. Given the completion time of the task, the trajectory of main UAV and the sensor transmission schedule are iteratively optimized to maximize the minimum amount of data uploaded by sensors. The simulation results verify the feasibility of the proposed algorithm in different application scenarios. For sub-problem 2, based on the trajectory of main UAV optimized by sub-problem 1, a particle swarm optimization (PSO)-based algorithm is designed to optimize the POPs of UAV and minimize the average positioning error of sensors. Furthermore, the spline curve is applied to generate the trajectory of auxiliary UAV. The simulation results show that the proposed scheme can achieve the meter-level positioning accuracy with only three UAVs.

The rest of this paper is organized as follows. Section II introduces the system model and the problem formulation.

In Section III, we propose an efficient optimization method to solve the mixed-integer non-convex optimization problem. In Section IV, the numerical simulation results are provided to verify the proposed scheme and evaluate its performance. Section V summarizes this paper.

II. SYSTEM MODEL AND PROBLEM FORMULATION

Consider a WSN with an area of $L \times L(m^2)$. There are M sensors randomly deployed in fixed positions to collect data from their surrounding environment, where the set of sensors is denoted by $\mathcal{M} = \{1, \dots, m, \dots, M\}$. Assume that the possible deployment space of sensors can be obtained from prior information. The real coordinates of sensors can be defined as $(s_m^T, h_m)^T$, with h_m being the vertical coordinate and

$$\mathbf{s}_m = (x_m^s, y_m^s)^T \in \mathbb{R}^{2 \times 1} \quad (1)$$

being the horizontal coordinate. Due to the portability and hovering ability, rotorcraft UAVs are adopted in this paper. Let $\mathcal{N} = \{1, \dots, n, \dots, N\}$ be the set of UAVs, including one main UAV and $N - 1$ auxiliary UAVs. Assume that UAVs start at $t = 0$ and fly at a fixed altitude H . The period for positioning and data collection is T . The horizontal coordinates of UAVs at $t \in [0, T]$ can be expressed as

$$\mathbf{u}_n(t) = (x_n^u(t), y_n^u(t))^T \in \mathbb{R}^{2 \times 1}. \quad (2)$$

The speed of UAVs can be denoted by the time-derivative of $\mathbf{u}_n(t)$

$$\mathbf{v}_n(t) \triangleq \dot{\mathbf{u}}_n(t), \quad (3)$$

where $\dot{\mathbf{u}}_n(t)$ is the derivative operation. To avoid unnecessary energy consumption, the sensor is generally in a sleep state. After receiving the activation signal from the UAV 1, the sensor will transmit the collected data to UAVs in the way of backscattering [29]. The task period is equally divided into W time slots of length τ with $\mathcal{W} = \{1, \dots, w, \dots, W\}$ being the index. The position and speed of UAVs and the channel environment between UAVs and sensors are stable in each time slot τ [27]. Based on path discrete method, the continuous trajectory of UAVs is divided into trajectory sequences. In the w -th time slot, the position and speed of the UAV can be expressed as $\mathbf{u}_n[w]$ and $\mathbf{v}_n[w]$, respectively.

A. Model of TDoA Localization

The positioning of sensors in WSN is usually implemented by using the TDoA algorithm, which has the advantages of low complexity and low time synchronization requirements [30]. Suppose that the synchronization accuracy between UAVs can meet the requirements of TDoA. As shown in Fig. 1, there are N UAVs to locate the sensor, where UAV 1 is used as the main UAV, and others are used as auxiliary UAVs. The actual TDoA of the positioning signal received by multiple time-synchronized UAVs is

$$t_{n1}^0 = t_n^0 - t_1^0, \quad i = 2, 3, \dots, N, \quad (4)$$

where t_n^0 is the ToA of the positioning signal from the sensor to the n -th UAV. The estimated location of the sensor can

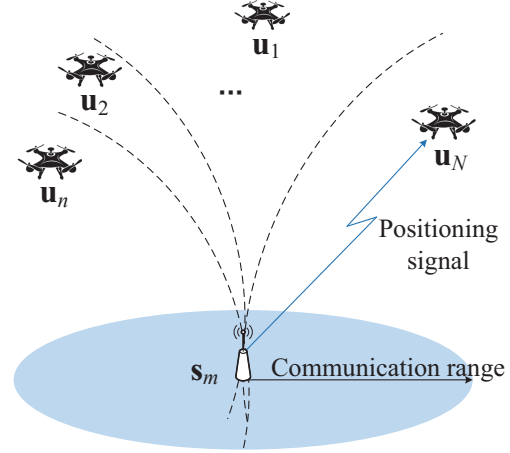


Fig. 1: TDoA positioning assisted by N UAVs.

be obtained by solving the hyperbolic equations composed of $N - 1$ observations below.

$$ct_{n1}^0 = r_n - r_1 = \sqrt{\|\mathbf{u}_n[w] - \mathbf{s}_m\|^2 + (H - h_m)^2} - \sqrt{\|\mathbf{u}_1[w] - \mathbf{s}_m\|^2 + (H - h_m)^2}, \quad i = 2, 3, \dots, N, \quad (5)$$

where c is the speed of electromagnetic wave. As Fig. 1 shows, the estimated position of the sensor is the intersection of multiple hyperbolas. At least three UAVs are required for two-dimensional (2D) positioning. Considering the random noise, the matrix of TDoA localization model can be expressed as

$$\mathbf{r} = \mathbf{r}^0 + \mathbf{e} = [ct_{21}^0, ct_{31}^0, \dots, ct_{N1}^0]^T + [e_{21}, e_{31}, \dots, e_{N1}]^T, \quad (6)$$

where $e_{n1} = c\Delta t_{n1}$ is the measurement error of the TDoA, and follows the zero mean Gaussian distribution with variance δ^2 . According to [31], the Cramer-Rao lower bound (CRLB) based on TDoA method is

$$\text{CRLB}(\mathbf{s}) = c^2 \text{trace} \left((\mathbf{H}\mathbf{Q}_t^{-1}\mathbf{H}^T)^{-1} \right), \quad (7)$$

where $\mathbf{Q}_t = \text{E}\{\mathbf{e}\mathbf{e}^T\}$ is the covariance matrix of the observed values of the TDoA. \mathbf{H} is the Jacobian matrix of the equation, which is expressed as

$$\mathbf{H} = \begin{bmatrix} \frac{\partial ct_{21}^0}{\partial x} & \dots & \frac{\partial ct_{N1}^0}{\partial x} \\ \frac{\partial ct_{21}^0}{\partial y} & \dots & \frac{\partial ct_{N1}^0}{\partial y} \end{bmatrix}, \quad (8)$$

The partial derivative $\partial ct_{i1}^0 / \partial x$ and $\partial ct_{i1}^0 / \partial y$ can be expressed as

$$\frac{\partial ct_{21}^0}{\partial x} = \frac{x_1^u - x_m^s}{r_1} - \frac{x_2^u - x_m^s}{r_2}, \quad (9)$$

$$\frac{\partial ct_{21}^0}{\partial y} = \frac{y_1^u - y_m^s}{r_1} - \frac{y_2^u - y_m^s}{r_2}. \quad (10)$$

Obviously, the positioning performance of the sensor assisted by UAVs is directly related to the position of UAVs. It is assumed that UAVs only select the position with the best performance as the POPs in their flight trajectory. Therefore, the trajectory design of UAVs is very important.

B. Model of Ground-to-Air Channel

Due to the flying altitude of the UAV, the communication between the UAV and the sensor is more likely to be dominated by the LoS link, especially in the environment with few obstacles [32], [33]. The impact of small-scale fading on signal attenuation is usually ignored in the scenario of UAV-assisted data collection [34], [35]. Therefore, we only consider the path loss in the ground-to-air (G2A) channel, and the channel gain from sensors to UAVs can be expressed as [36]

$$\begin{aligned} PL_m[w] &= \beta_0 d_m^{-\alpha}[w] \\ &= \beta_0 \left(\|\mathbf{u}_1[w] - \mathbf{s}_m\|^2 + (H - h_m)^2 \right)^{-\alpha/2}, \end{aligned} \quad (11)$$

where β_0 is the free space path loss at the reference distance of 1 m, and $\alpha \geq 2$ is the path loss factor. $\mathbf{u}_1[w]$ and \mathbf{s}_m represent the position of UAV 1 and sensor m in the w -th time slot, respectively.

Specifically, the UAV 1 can establish communication links with at most K_{\max} ($1 \leq K_{\max} \leq M$) sensors and receive data in each time slot. The bandwidth B_0 is evenly divided into K sensors to upload data at the same time, and the set of connected sensors denoted by \mathcal{K} . Then the bandwidth allocated to each sensor is

$$B[w] = \frac{B_0}{K}. \quad (12)$$

The signal to interference plus noise ratio (SINR) between the sensor m and UAV 1 can be expressed as

$$\gamma_m[w] = \frac{P_t \cdot PL_m[w]}{\sum_{k \in \mathcal{K} \setminus m} P_t \cdot PL_m[w] + \sigma^2}, \quad (13)$$

where P_t is the fixed transmission power of the sensor, $\sum_{k \in \mathcal{K} \setminus m} P_t \cdot PL_m[w]$ is the co-channel interference, and σ^2 is the power of additive Gaussian white noise (AWGN). If the UAV 1 serves the sensor in the w -th time slot, the transmission rate (bits/s) can be expressed as [37], [38]

$$R_m[w] = B[w] \log_2(1 + \gamma_m[w]). \quad (14)$$

The wake-up communication scheduling method is adopted in this paper [35], [39]. The schedule of the transmission can be controlled to determine the sensor to communicate in each time slot. Assume that the UAV 1 can only collect data from one sensor in a time slot, i.e., $K_{\max} = 1$. Define a binary variable $x_m[w], \forall m, w$ to represent data transmission in WSN. $x_m[w] = 1$ denotes that sensor m transmits data to UAV 1 in the w -th time slot, while $x_m[w] = 0$ denotes the reverse process. Therefore, we have the following transmission schedule constraints.

$$x_m[w] \in \{0, 1\} \quad \forall m \in \mathcal{M}, w \in \mathcal{W}, \quad (15)$$

$$\sum_{m=1}^M x_m[w] \leq 1 \quad \forall w \in \mathcal{W}. \quad (16)$$

Furthermore, the amount of data uploaded by sensor m in the whole task is

$$I_m = \tau \sum_{w=1}^W R_m[w] \cdot x_m[w] \quad \forall m \in \mathcal{M}. \quad (17)$$

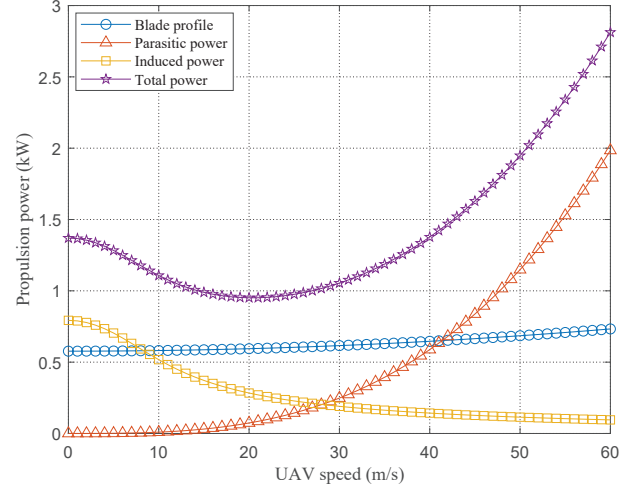


Fig. 2: Propulsion powers versus UAV speed.

Algorithm 1 BCD for sub-problem 1

- 1: **Initialize** $\{\mathbf{u}_1^0[w]\}$, \mathbf{X}^0 and let $l \leftarrow 0$.
 - 2: **repeat**
 - 3: For given $\{\mathbf{u}_1^l[w]\}$, solve (sP1-1) and denote the optimal solution as \mathbf{X}^{l+1} .
 - 4: For given \mathbf{X}^{l+1} , solve (sP1-4) and denote the optimal solution as $\{\mathbf{u}_1^{l+1}[w]\}$.
 - 5: $l \leftarrow l + 1$.
 - 6: **until** $l = l_{\max}$.
-

According to (14) and (17), it is revealed that the data transmission rate is directly related to the distance between the UAV and the sensor, namely, the instantaneous position of UAV 1 when collecting data will affect the efficiency of data collection. Therefore, it is necessary to design reasonable transmission schedule and UAV trajectory to ensure the performance of data collection.

C. Model of UAV Energy Consumption

The energy consumption of UAV is mainly divided into two parts: communication energy consumption (signal transmission, reception and processing) and propulsion energy consumption (flying and hovering). Since the propulsion energy consumption is usually much larger than communication energy consumption, the communication energy consumption can be ignored [40]. According to [41], when the UAV flies at speed $\mathbf{v}_n[w]$, the propulsion energy consumption has three

components, which can be modeled as

$$P(\mathbf{v}_n[w]) = \underbrace{k_b \left(1 + \frac{3\|\mathbf{v}_n[w]\|^2}{v_t^2} \right)}_{\text{Blade profile}} + \underbrace{\frac{1}{2}\rho s d_r A \|\mathbf{v}_n[w]\|^3}_{\text{Parasitic power}} + \underbrace{k_i \left(\sqrt{1 + \frac{\|\mathbf{v}_n[w]\|^4}{4v_0^4}} - \frac{\|\mathbf{v}_n[w]\|^2}{2v_0^2} \right)^{1/2}}_{\text{Induced power}}, \quad (18)$$

where k_b and k_i are the blade profile power and induced power when the UAV hovers respectively. ρ is the air density, s is the rotor solidity, d_r is the drag coefficient of UAV and A is the rotor surface area. v_t and v_0 are the blade tip speed and mean rotor induced speed in hovering respectively. When $\mathbf{v}_n[w] = \mathbf{0}^T$, the hovering power of UAV can be obtained as $P_h = k_b + k_i$. Fig. 2 shows the curve of total power and three power components as the rate changes.

D. Problem Formulation

Define $\mathbf{U} = \{\mathbf{u}_n[w], \forall n, w\}$ and $\mathbf{X} = \{x_m[w], \forall m, w\}$. To jointly optimize the UAV trajectory \mathbf{U} and sensor transmission scheduling \mathbf{X} , we need to minimize the average positioning error of sensors, while ensuring the successful data uploading. Then, the optimization problem can be formulated as

$$(P0): \min_{\mathbf{X}, \mathbf{U}} \frac{\sum_{m=1}^M \text{CRLB}_m(\mathbf{u}_1[w], \dots, \mathbf{u}_n[w])}{M} \quad (19)$$

$$\text{s.t. } \tau \sum_{w=1}^W P(\|\mathbf{v}_n[w]\|) \leq E_{\max}, \quad \forall n \in \mathcal{N}, \quad (19a)$$

$$x_m[w] \in \{0, 1\}, \quad \forall m \in \mathcal{M}, w \in \mathcal{W}, \quad (19b)$$

$$\sum_{m=1}^M x_m[w] \leq 1, \quad \forall w \in \mathcal{W}, \quad (19c)$$

$$\tau \sum_{w=1}^W R_m[w] \cdot x_m[w] \geq I_{\min}, \quad \forall m \in \mathcal{M}, \quad (19d)$$

$$\|\mathbf{u}_n[w] - \mathbf{u}_n[w-1]\| \leq \tau V_{\max}, \quad \forall n \in \mathcal{N}, w \in \mathcal{W}, \quad (19e)$$

$$\|\mathbf{u}_i[w] - \mathbf{u}_1[w]\| \leq R_{\max}, \quad \forall w \in \mathcal{W}, i \neq 1, \quad (19f)$$

$$\mathbf{u}_n[0] = \mathbf{u}_s, \mathbf{u}_n[W] = \mathbf{u}_e, \quad \forall n \in \mathcal{N}, \quad (19g)$$

where V_{\max} is the maximum speed of UAVs, R_{\max} is the maximum communication distance between the auxiliary UAV and UAV 1. (19a) is the constraint of maximum flight energy consumption of UAVs. (19b) limits the feasible range of optimization variable \mathbf{X} , and (19c) ensures that the number of sensors accessing UAV 1 at the same time does not exceed 1. (19d) ensures that the amount of data uploaded by each sensor can meet the requirements. (19e) is the constraint of maximum flight speed. (19f) represents the communication performance limitations of UAVs respectively, which ensures that the auxiliary UAV can maintain communication with UAV 1 during positioning. (19g) represents the start and end points

of UAV trajectories. The UAV cannot collect a large amount of data with extremely low energy. In practical applications, the values of E_{\max} and I_{\min} can be continuously adjusted to ensure that at least one solution simultaneously satisfies all constraints [42].

Note that the calculation of data transmission rate and CRLB both requires the accurate position of the sensor in problem (P0). Therefore, we build the uncertainty model of the sensor by making a circle with rough position as the center and uncertainty parameter as the radius [27]. By assuming that the sensor is located at the farthest distance from UAV 1 in the model, each sensor can upload enough data when the data transmission rate is the lowest. In the same way, when estimating the location of the sensor, multiple sampling points are scattered in the uncertainty model to calculate the CRLB, and the points with maximum value are selected as the POPs.

This model is also suitable for scenarios with optimization requirements for flight altitude of UAVs. Some constraints on the vertical trajectory need to be added, i.e. [43], [44],

$$\|H_n[w] - H_n[w-1]\| \leq \tau V_{z-\max}, \quad \forall n \in \mathcal{N}, w \in \mathcal{W}, \quad (20)$$

$$H_n[0] = H_s, H_n[W] = H_e, \quad \forall n \in \mathcal{N}, \quad (21)$$

$$H_{\min} \leq H_n[w] \leq H_{\max}, \quad \forall n \in \mathcal{N}, w \in \mathcal{W}, \quad (22)$$

where (20) is the constraint of the vertical flight speed. (21) and (22) constrain the flight height of UAVs within each time slot. Besides, considering the three-dimensional (3D) trajectory, the constraint (19f) needs to be rewritten as

$$\|\mathbf{u}_i[w] - \mathbf{u}_1[w]\|^2 + \|H_n[w] - H_n[w-1]\|^2 \leq R_{\max}^2, \quad \forall w \in \mathcal{W}, i \neq 1. \quad (23)$$

However, the modification of (19a) is the main challenge in building and solving the 3D model. On the one hand, in 3D scenarios, the model of energy consumption needs to consider more factors, such as the changing lift and drag of the UAV [45], [46], [41]. On the other hand, more complex formulas result in a change in the problem structure, which means that the optimization problem is difficult to convert into a convex problem to solve.

III. PROPOSED OPTIMIZATION METHOD

The optimization problem (P0) involves infinite variables, binary constraints and non-convex constraints, and the objective function is not a closed-form expression. Therefore, (P0) is a mixed-integer non-convex optimization problem, which is difficult to find the optimal solution directly. According to the analysis in Section II, the transmission rate in data collection is affected by the distance between the UAV 1 and the sensor, while the CRLB for sensor positioning is related to the relative position of all UAVs and the sensor. Therefore, we divide original problem (P0) into two sub-problems. In sub-problem (sP1), we optimize the trajectory of UAV 1 and the transmission schedule of sensors to maximize the amount of data uploaded. In sub-problem (sP2), based on the trajectory points of UAV 1, a PSO-based optimization method is designed to determine the optimal POPs of UAVs and minimize the average CRLB. Furthermore, the trajectories

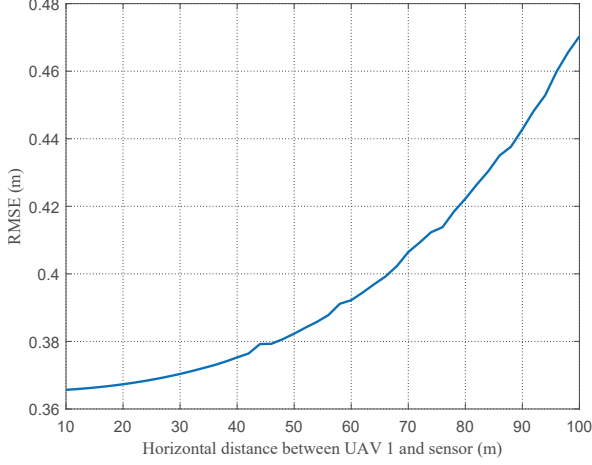


Fig. 3: RMSE versus the distance between UAV 1 and the sensor.

of auxiliary UAVs are generated by spline curve. The solution obtained using the above is approximately optimal, but has lower complexity.

A. (sP1): Transmission Scheduling and UAV 1 Trajectory Optimization

For sub-problem (sP1), we apply alternating iteration technique to optimize the transmission scheduling of sensors and the trajectory of UAV 1, i.e., \mathbf{X} and $\mathbf{u}_1[w]$. The details of BCD method are summarized in Algorithm 1. Sub-problem (sP1) can be formulated as

$$(sP1): \max_{\lambda, \mathbf{X}, \{\mathbf{u}_1[w]\}} \lambda \quad (24)$$

$$\text{s.t. } \tau \sum_{w=1}^W P(\|\mathbf{v}_1[w]\|) \leq E_{\max}, \quad (24a)$$

$$x_m[w] \in \{0, 1\}, \quad \forall m \in \mathcal{M}, w \in \mathcal{W}, \quad (24b)$$

$$\sum_{m=1}^M x_m[w] \leq 1, \quad \forall w \in \mathcal{W}, \quad (24c)$$

$$\frac{\tau}{I_{\min}} \sum_{w=1}^W R_m[w] \cdot x_m[w] \geq \lambda, \quad \forall m \in \mathcal{M}, \quad (24d)$$

$$\|\mathbf{u}_1[w] - \mathbf{u}_1[w-1]\| \leq \tau V_{\max}, \quad \forall n \in \mathcal{N}, w \in \mathcal{W}, \quad (24e)$$

$$\mathbf{u}_1[0] = \mathbf{u}_s, \mathbf{u}_1[W] = \mathbf{u}_e, \quad \forall n \in \mathcal{N}, \quad (24f)$$

where λ is the slack variable. To simplify the mixed-integer non-convex problem, we first slacken the constraint (24b) to $0 \leq x_m[w] \leq 1, \forall m \in \mathcal{M}, w \in \mathcal{W}$. Each time slot is divided into Z time blocks. Then, for any given trajectory $\mathbf{u}_1[w]$, the transmission scheduling \mathbf{X} can be obtained by solving the following problem.

$$(sP1-1): \max_{\lambda, \mathbf{X}} \lambda \quad (25)$$

$$\text{s.t. } 0 \leq x_m[w] \leq 1, \quad \forall m \in \mathcal{M}, w \in \mathcal{W}, \quad (25a)$$

Algorithm 2 Proposed PSO-based for sub-problem 2

- 1: **Input:** Trajectory $\{\mathbf{u}_1[w]\}$ and altitude H of UAV 1, number of sensors M , number of UAVs N , parameters of sensor position uncertainty (h, \tilde{s}_m and r_u), maximum iterations r_{\max} , population size N_p in the PSO-based algorithm.
- 2: **Initialization:**
- 3: Obtain the UAV 1 POPs \mathbf{I}_1^* according to the parameters.
- 4: Initialize the position vector $\mathbf{P}^0 = \{\mathbf{P}_1^0, \dots, \mathbf{P}_{N_p}^0\}$ and velocity vector $\mathbf{V}^0 = \{\mathbf{V}_1^0, \dots, \mathbf{V}_{N_p}^0\}$ of the particle swarm. The position of each particle \mathbf{P}_i^0 is a set of distances and angles to determine the POPs of the auxiliary UAV.
- 5: Calculate the fitness $f(\mathbf{P}_i^0)$ for each particle, whose reciprocal is the average positioning error e_i^0 .
- 6: Set the historical optimal position of each particle $\mathbf{Pbest}_i \leftarrow \mathbf{P}_i^0$.
- 7: Obtain the global optimal position of particle swarm. Find $i^* = \arg \max_{i \in \{1, \dots, N_p\}} \{f(\mathbf{Pbest}_i)\}$, and set $\mathbf{Gbest}^0 \leftarrow \mathbf{Pbest}_{i^*}$.
- 8: Set the optimal particle $\mathbf{P}^* \leftarrow \mathbf{Gbest}^0$ and corresponding fitness f^* .
- 9: $r \leftarrow 0$.
- 10: **Repeat:**
- 11: Update the velocity vector $\mathbf{V}^{r+1} = \{\mathbf{V}_1^{r+1}, \dots, \mathbf{V}_{N_p}^{r+1}\}$ and position vector $\mathbf{P}^{r+1} = \{\mathbf{P}_1^{r+1}, \dots, \mathbf{P}_{N_p}^{r+1}\}$ of the population.
- 12: Calculate the fitness $f(\mathbf{P}_i^{r+1})$ for each particle.
- 13: For each particle, if $f(\mathbf{P}_i^{r+1}) > f(\mathbf{Pbest}_i)$: $\mathbf{Pbest}_i \leftarrow \mathbf{P}_i^{r+1}$.
- 14: Find $i^* = \arg \max_{i \in \{1, \dots, N_p\}} \{f(\mathbf{Pbest}_i)\}$, and set $\mathbf{Gbest}^{r+1} \leftarrow \mathbf{Pbest}_{i^*}$.
- 15: If $f(\mathbf{Gbest}^{r+1}) > f(\mathbf{P}^*)$: $\mathbf{P}^* \leftarrow \mathbf{Gbest}^{r+1}$.
- 16: **until** $r = r_{\max}$.
- 17: Calculate auxiliary UAV POPs $\{\mathbf{I}_2^*, \dots, \mathbf{I}_N^*\}$ according to \mathbf{P}^* .
- 18: $\mathbf{I}^* = \{\mathbf{I}_1^*, \dots, \mathbf{I}_N^*\}$ and minimum average positioning error e^* .

$$(24c), (24d).$$

Problem (sP1-1) is a standard linear programming (LP), which can be simply solved. For given \mathbf{X} , $\mathbf{u}_1[w]$ is optimized to maximize the minimum amount of data. Specifically, the problem can be expressed as

$$(sP1-2): \max_{\lambda, \{\mathbf{u}_1[w]\}} \lambda \quad (26)$$

$$\text{s.t. } (24a), (24d), (24e), (24f).$$

Due to constraints (24a) and (24d), (sP1-2) is still a non-convex optimization problem. To deal with the non-convex constraint (24a), the variable $\varsigma[w] \geq 0$ is introduced. Let $\varsigma[w] = \left(\sqrt{1 + \frac{\|\mathbf{v}_1[w]\|^4}{4v_0^4}} - \frac{\|\mathbf{v}_1[w]\|^2}{2v_0^2} \right)^{1/2}$, i.e., $\frac{1}{\varsigma[w]^2} = \varsigma[w]^2 +$

$$A_1^l [w] = \log_2 \left(1 + \frac{c_0}{\left(\|\mathbf{u}_1^l [w] - \mathbf{s}_m\|^2 + (H - h_m)^2 \right)^{\alpha/2}} \right) \quad (23)$$

$$A_2^l [w] = \frac{\alpha c_0 \log_2 e / 2}{\left(\|\mathbf{u}_1^l [w] - \mathbf{s}_m\|^2 + (H - h_m)^2 \right) \left(\left(\|\mathbf{u}_1^l [w] - \mathbf{s}_m\|^2 + (H - h_m)^2 \right)^{\alpha/2} + c_0 \right)} \quad (24)$$

$\frac{\|\mathbf{v}_1[w]\|^2}{v_0^2}$ [42]. Then, problem (sP1-2) is transformed into

$$(sP1-3) : \max_{\lambda, \{\mathbf{u}_1[w]\}, \{\varsigma[w]\}} \lambda \quad (27)$$

$$\text{s.t. } \tau \sum_{w=1}^W P(\|\mathbf{v}_1[w]\|, \varsigma[w]) \leq E_{\max}, \quad (27a)$$

$$\varsigma[w]^2 + \frac{\|\mathbf{v}_1[w]\|^2}{v_0^2} \geq \frac{1}{\varsigma[w]^2}, \quad \forall w \in \mathcal{W}, \quad (27b)$$

(24d), (24e), (24f).

where

$$P(\|\mathbf{v}_1[w]\|, \varsigma[w]) = k_b \left(1 + \frac{3\|\mathbf{v}_1[w]\|^2}{v_t^2} \right) + \frac{1}{2} \rho s d_r A \|\mathbf{v}_1[w]\|^3 + k_i \varsigma[w], \quad (28)$$

$$R_m[w] = B \log_2 \left(1 + \frac{c_0}{\left(\|\mathbf{u}_1[w] - \mathbf{s}_m\|^2 + (H - h_m)^2 \right)^{\frac{\alpha}{2}}} \right), \quad (29)$$

where $c_0 = P_t \beta_0 / \sigma^2$. According to [42], problems (sP1-2) and (sP1-3) are equivalent. To obtain an effective approximate solution, we use SCA technique to transform the problem into a series of convex problems, and maximize the lower bound of (sP1-3). Let $R_m^l[w]$ be the first-order Taylor expansion of $R_m[w]$ on feasible point $\mathbf{u}^l \triangleq \|\mathbf{u}_1[w] - \mathbf{s}_m\|^2$ in the l -th iteration. Then,

$$R_m[w] \geq R_m^l[w] \triangleq B A_1^l[w] - B A_2^l[w] \|\mathbf{u}_1[w] - \mathbf{s}_m\|^2 + B A_2^l[w] \|\mathbf{u}_1^l[w] - \mathbf{s}_m\|^2, \quad (30)$$

where the formulas of $A_1^l[w]$ and $A_2^l[w]$ are shown in (23) and (24) respectively. Similarly, for the first-order Taylor expansion of (27b) at $\varsigma^l[w]$ and $\mathbf{v}_1^l[w]$,

$$\begin{aligned} \varsigma[w]^2 + \frac{\|\mathbf{v}_1[w]\|^2}{v_0^2} &\geq \vartheta^l[w] \triangleq -\varsigma^l[w]^2 + 2\varsigma^l[w]\varsigma[w] \\ &\quad - \frac{\|\mathbf{v}_1^l[w]\|^2}{v_0^2} + \frac{2}{v_0^2} \|\mathbf{v}_1^l[w]\| \cdot \|\mathbf{v}_1[w]\|. \end{aligned} \quad (25)$$

By introducing the lower bound $R_m^l[w]$ and $\vartheta^l[w]$, problem (sP1-3) can be approximated as follows in the l -th iteration.

$$(sP1-4) : \max_{\lambda, \{\mathbf{u}_1[w]\}, \{\varsigma[w]\}} \lambda \quad (26)$$

$$\text{s.t. } \vartheta^l[w] \geq \frac{1}{\varsigma[w]^2}, \quad \forall w \in \mathcal{W}, \quad (26a)$$

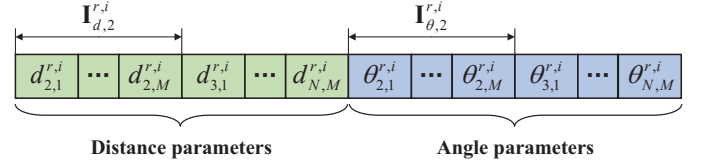


Fig. 4: Composition of the i -th particle \mathbf{P}_i^r in the r -th iteration.

$$\frac{\tau}{I_m} \sum_{w=1}^W R_m^l[w] \cdot x_m[w] \geq \lambda, \quad \forall m \in \mathcal{M}, \quad (26b)$$

(27a), (24e), (24f).

Problem (sP1-4) is a convex optimization problem, which can be solved by CVX. To sum up, by solving problems (sP1-1) and (sP1-4) alternately, we can obtain a local optimal solution of (sP1).

B. (sP2): PoPs and Auxiliary UAV Trajectory Optimization

Based on the optimal UAV 1 trajectory obtained in (sP1), we can find the trajectories of auxiliary UAVs that meet the positioning requirements. However, the objective function of (sP2) does not have a closed-form expression, which is difficult to be solved by conventional optimization methods. To simplify the problem and obtain a feasible solution, we propose a PSO-based algorithm to optimize POPs of UAVs. The detailed process is shown in Algorithm 2, and the obtained solution is local optimal. To select the POPs of UAV 1, we first explore the effect of the distance between UAV 1 and the sensor on the positioning performance. As shown in Fig. 3, the RMSE of the sensor almost linearly increases with the horizontal distance changes from 10 m to 100 m. Therefore, the UAV 1 position nearest to the sensor is selected as the POP.

In the PSO algorithm, particles have two attributes: position and velocity. The position is considered as a candidate solution of the optimization problem. In a iteration, the particle tracks the extreme values of its individual and entire population in the search space and adjusts its position and velocity to find a satisfactory solution. Since the auxiliary UAVs needs to be within the communication range of UAV 1 during positioning, we define the position vector of each particle as the set of the distance and angle between the auxiliary UAV and UAV 1, as shown in Fig. 4. Among them, $\mathbf{I}_{d,2}^{r,i}$ and $\mathbf{I}_{\theta,2}^{r,i}$ represent the distance and angle of the auxiliary UAV 2 relative to UAV 1 at the POP, respectively. The distance parameter meets the constraint of communication range, namely $d_{n,m}^{r,i} \leq R_{\max}$.

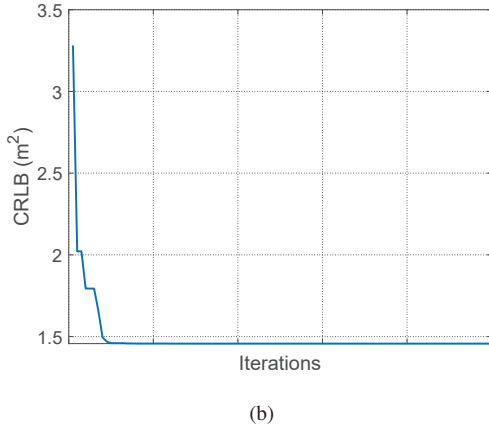
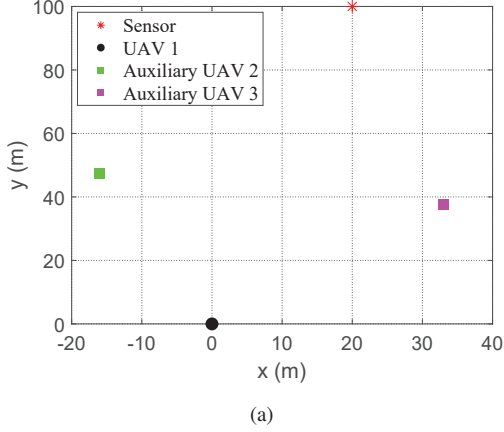


Fig. 5: POPs Optimization using the proposed PSO-based algorithm with $N = 3$ and $R_{\max} = 50$ m. (a)The optimal POPs. (b)Corresponding iterative curve.

To minimize the average positioning error of M sensors while satisfying the constraints (19a) and (19e), we set the following fitness function [27].

$$fit(\mathbf{P}_i^l) = \frac{1}{c_{\text{CRLB}} f_{\text{CRLB}} + c_e f_e + c_v f_v}, \quad (27)$$

where f_e and f_v are binary variables and represent the penalty items of energy consumption and speed constraints. f_{CRLB} is the average CRLB of all sensors. When the above constraint is violated, let $f_e = 0$ or $f_v = 0$. c_{CRLB} , c_e and c_v are the corresponding penalty factors, and the values of c_e and c_v should be much greater than the values of c_{CRLB} , so as to give the infeasible particle a lower fitness value. (27) ensures that the optimal solution obtained in each iteration is feasible.

To balance the global search ability and local search ability of the algorithm, we adopt the strategy of inertia weight linearly decreasing, as shown in (28).

$$\omega^r = \omega_{\max} - \frac{(\omega_{\max} - \omega_{\min})r}{r_{\max}}, \quad (28)$$

where ω^r is the linearly decreasing adaptive inertia weight, and r is the current iteration number. ω_{\max} and ω_{\min} are the final and initial values of inertia weight respectively, with typical values of 0.9 and 0.4 [47]. With the increasing of

TABLE I: Simulation parameters

Parameter	Value
Length of target area (L)	1 km
Number of UAVs (N)	3
Number of sensors (M)	5
UAV flight altitude (H)	100 m
Sensor height (h_m)	0 m
Number of time slots (W)	100
Length of time slots (τ)	1 s
Carrier frequency (f)	2.1 GHz
Channel bandwidth (B_0)	1 MHz
Reference channel power gain at 1 m (β_0)	-60 dB
Path loss factor (α)	2
Noise power (δ^2)	-110 dBm
Transmit power of sensors (P_t)	0.1 W
Maximum speed of UAVs (V_{\max})	30 m/s
Maximum communication range between UAVs (R_{\max})	50 m
Maximum number of sensors communicating with UAV (K_{\max})	1
Radius of uncertainty location area (r_u)	10 m
amount of data uploaded by each sensor (I_{\min})	20 Mbits
Initial position of UAVs (\mathbf{u}_s)	$(0, 0)^T$ m
Final position of UAVs (\mathbf{u}_e)	$(1000, 0)^T$ m
Population size (N_p)	50
Maximum iterations of BCD algorithm (l_{\max})	30
Maximum iterations of PSO algorithm (r_{\max})	200

iterations, ω^r decreases gradually, and the global search ability and local search ability of PSO are weakened and enhanced respectively. The particle updates itself by tracking the optimal solution found by itself (individual extremum \mathbf{Pbest}_i^r) and the optimal solution found by the whole population (global extremum \mathbf{Gbest}^r). Each particle updates its speed and position according to (29) and (30).

$$\mathbf{V}_i^{r+1} = \underbrace{\omega^r \mathbf{V}_i^r}_{\text{Memory item}} + \underbrace{c_1 \cdot rand() \cdot (\mathbf{Pbest}_i^r - \mathbf{P}_i^r)}_{\text{Self-cognition item}} + \underbrace{c_2 \cdot rand() \cdot (\mathbf{Gbest}^r - \mathbf{P}_i^r)}_{\text{Group-cognition item}}, \quad (29)$$

$$\mathbf{P}_i^{r+1} = \mathbf{P}_i^r + \mathbf{V}_i^{r+1}, \quad (30)$$

where c_1 and c_2 are learning factors, $rand()$ is a random number between 0 and 1, and \mathbf{V}_i^r and \mathbf{P}_i^r are the velocity and position of the i -th particle with certain limits. When the values \mathbf{V}_i^r and \mathbf{P}_i^r are outside the feasible range, they will be assigned to the minimum or maximum values within the feasible range.

To verify the feasibility of the proposed algorithm, a simple scenario is designed for testing. We set $\mathbf{u}_1 = [0, 0]$ and $\mathbf{s} = [20, 100]$, and the optimal POPs of UAVs is shown in Fig. 5(a). Fig. 5(b) shows the CRLB decreases significantly with the number of iterations increases.

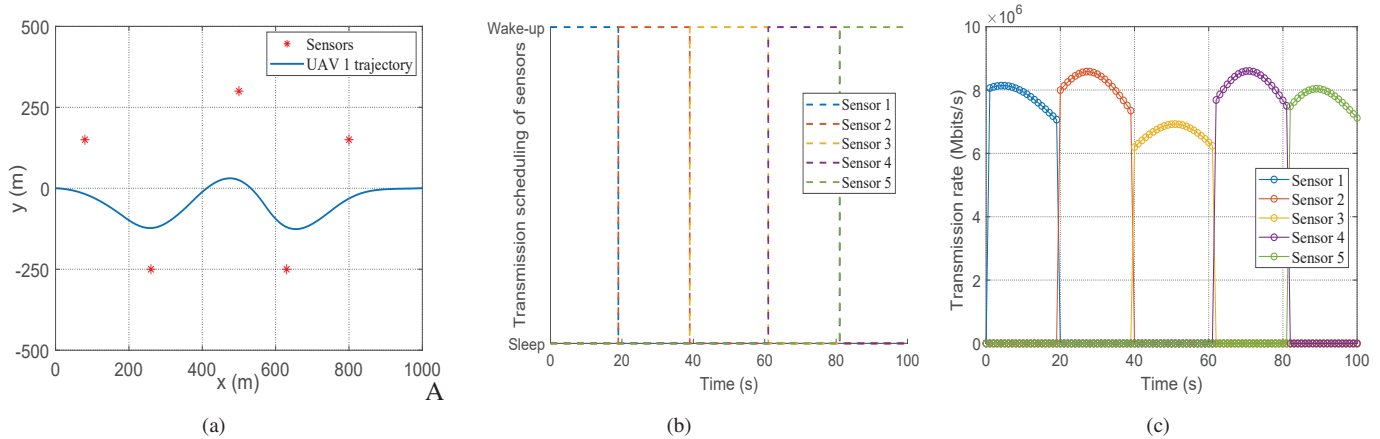


Fig. 6: Optimized (a) UAV 1 trajectory, (b) sensor transmission scheduling and (c) data transmission rate in scenario 1.

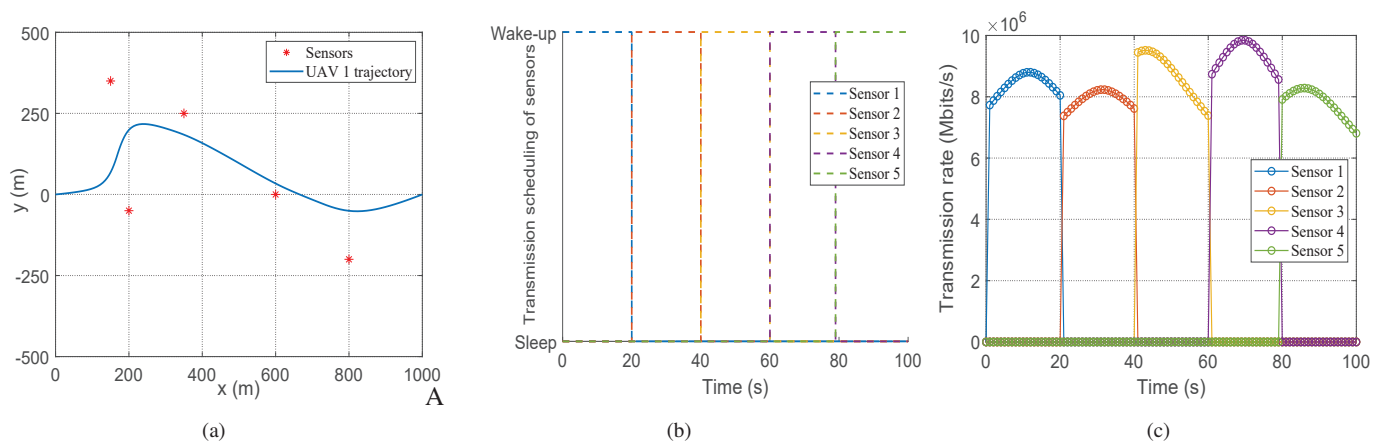


Fig. 7: Optimized (a) UAV 1 trajectory, (b) sensor transmission scheduling and (c) data transmission rate in scenario 2.

IV. NUMERICAL RESULTS

In this section, a series of numerical simulation results are provided to verify the proposed scheme and evaluate its performance. The key simulation parameters are summarized in Table I [42], [39], [27], [41].

A. Performance Evaluation of Data Collection

Fig. 6 and Fig. 7 show the optimized trajectory of UAV 1, sensor transmission scheduling and instantaneous data transmission rate with $E_{\max} = 700$ KJ under the two sensor deployment scenarios. Obviously, the trajectory of UAV 1 in Fig. 6(a) and Fig. 7(a) tends to be close to the sensor, and the sensor with relatively close distance is selected for data collection. This is due to the fact that the channel quality is high when the sensor is close. The above conclusion is also confirmed by the change of data transmission rate in Fig. 6(b) and Fig. 7(b). Fig. 6(c) and Fig. 7(c) show that the sensor will remain in sleep state until UAV 1 approaches it and wakes it up, and the communication time with each sensor is roughly the same. In addition, in order to maximize the minimum amount of data uploaded by the sensor, the UAV

1 will always maintain a communication link with the sensor without restricting the energy consumption of the sensor.

Fig. 8 shows the optimized trajectory of UAV 1 in the horizontal direction when the mission cycle T is 50 s, 100 s and 200 s respectively. As expected, with the increase of T , UAV 1 tends to be closer to sensors to improve the efficiency of data collection. The amount of data uploaded by each sensor and the average amount of data with different T are shown in Fig. 9. Through the trend of the total data amount, it can also be found that the sensors close to the flight trajectory can always upload more data.

Fig. 10 and Fig. 11 show the impact of energy consumption constraint on the trajectory and speed of UAVs. Given $T = 100$ s, as available energy increase, UAV 1 tends to fly at a higher rate to obtain a longer trajectory, which is consistent with the expected results. It is noted that the trajectories under $E_{\max} = 500$ KJ and $E_{\max} = 700$ KJ are very similar. Fig. 11 also shows that the trends of speed change in both cases is also roughly the same. When $E_{\max} = 700$ KJ, the average rate is higher, resulting in higher energy consumption.

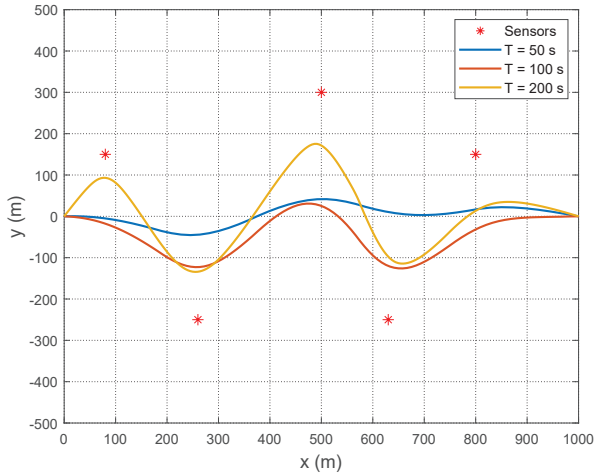


Fig. 8: Optimized UAV 1 trajectories with different T .

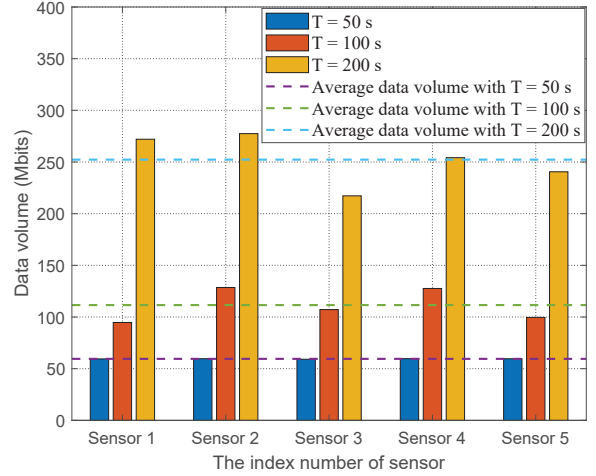


Fig. 9: The amount of data uploaded by each sensor and the average data amount.

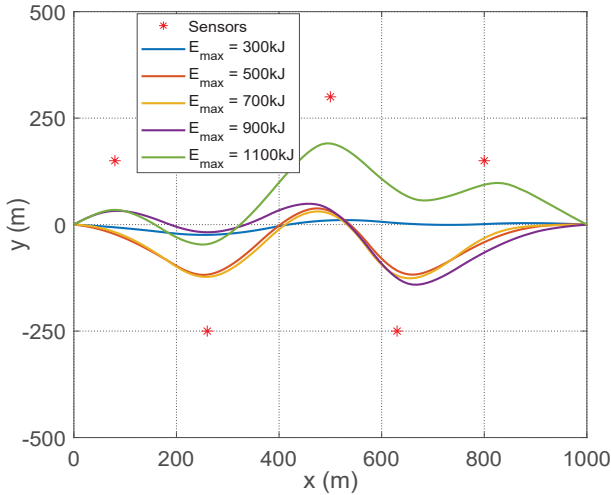


Fig. 10: Optimized UAV 1 trajectories for different E_{\max} .

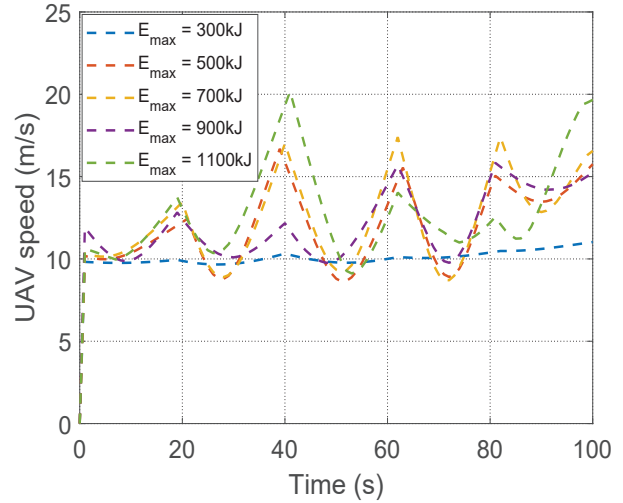
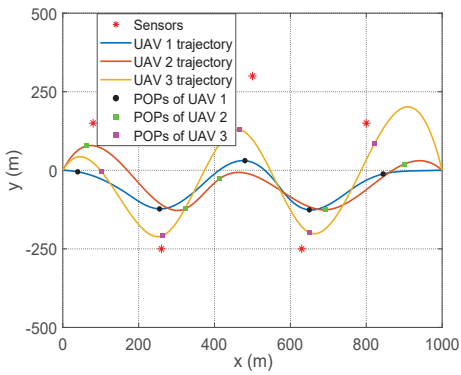
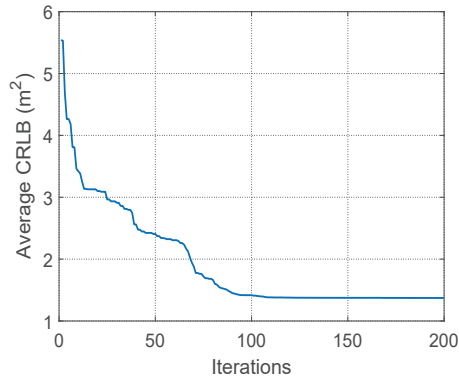


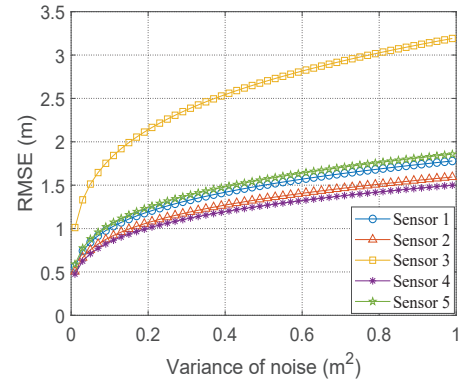
Fig. 11: Optimized UAV 1 speed for different E_{\max} .



(a)



(b)



(c)

Fig. 12: Application results of the proposed PSO-based algorithm. (a) Optimized UAV trajectories and POPs. (b) Corresponding iterative curve. (c) Influence of noise on positioning accuracy.

B. Performance Evaluation of Sensor Positioning

Fig. 12(a) shows the POPs and trajectories of auxiliary UAV obtained by Algorithm 2 based on the optimized trajectory of UAV 1 with $T = 100$ s and $E_{\max} = 700$ KJ. It is shown that in order to improve the positioning accuracy, UAVs are distributed as far as possible within the maximum communication range, which is consistent with the assumption. As shown in Fig. 12(b), as the number of iterations increases, the fitness of the optimal individual of the particle population continues to improve, and the average positioning error of the sensor decreases significantly.

The positioning at the POPs that are obtained in Fig. 12(a) is executed to study the relation between the positioning error and the variance of noise. As shown in Fig. 12(c), with the increase of the variance of noise, the positioning error of sensor shows a logarithmic growth trend. When the sensor is far from the anchor node, its positioning error is significantly higher than other sensors. This phenomenon inspires us to make the UAV 1 close to the sensor, so as to improve the positioning accuracy by increasing the signal-noise ratio (SNR) threshold.

V. CONCLUSION

This paper proposes a joint data collection and sensor positioning scheme for WSN using multiple UAVs. Firstly, the CRLB of sensor positioning with TDoA is derived to evaluate positioning performance. Then, a mixed-integer non-convex optimization model is established considering the constraints of the flight energy consumption, flight speed, requirements for data collection and communication range. The optimization model is to optimize the UAV flight trajectory, sensor transmission schedule and POPs jointly to minimize the average positioning error of sensors, while ensuring the amount of data collection. Then, BCD, SCA and PSO-based optimization algorithms are applied to solve the optimization model. The numerical simulation results show that the proposed scheme achieves efficient and reliable data collection, and have a good positioning performance. This paper may motivate the joint design of data collection and sensor positioning for WSN deployed in the areas that lack infrastructure coverage.

REFERENCES

- [1] L. Liu, S. Hua, and Q. Lai, "Automatic control system of balancing agricultural stereo cultivation based on wireless sensors," *IEEE Sensors Journal*, vol. 21, no. 16, pp. 17 517–17 524, 2021.
- [2] G. Tabella, N. Paltrinieri, V. Cozzani, and P. S. Rossi, "Wireless sensor networks for detection and localization of subsea oil leakages," *IEEE Sensors Journal*, vol. 21, no. 9, pp. 10 890–10 904, 2021.
- [3] X. Li, M. Sun, Y. Ma, L. Zhang, Y. Zhang, R. Yang, and Q. Liu, "Using sensor network for tracing and locating air pollution sources," *IEEE Sensors Journal*, vol. 21, no. 10, pp. 12 162–12 170, 2021.
- [4] A. Boubrima, W. Bechkit, and H. Rivano, "Optimal wsn deployment models for air pollution monitoring," *IEEE Transactions on Wireless Communications*, vol. 16, no. 5, pp. 2723–2735, 2017.
- [5] X. Li, J. Tan, A. Liu, P. Vijayakumar, N. Kumar, and M. Alazab, "A novel uav-enabled data collection scheme for intelligent transportation system through uav speed control," *IEEE Transactions on Intelligent Transportation Systems*, vol. 22, no. 4, pp. 2100–2110, 2021.
- [6] Z. Wei, M. Zhu, N. Zhang, L. Wang, Y. Zou, Z. Meng, H. Wu, and Z. Feng, "Uav-assisted data collection for internet of things: A survey," *IEEE Internet of Things Journal*, vol. 9, no. 17, pp. 15 460–15 483, 2022.
- [7] W. Chen, S. Zhao, R. Zhang, Y. Chen, and L. Yang, "Uav-assisted data collection with nonorthogonal multiple access," *IEEE Internet of Things Journal*, vol. 8, no. 1, pp. 501–511, 2021.
- [8] J. Grigulo and L. B. Becker, "Experimenting sensor nodes localization in wsn with uav acting as mobile agent," in *2018 IEEE 23rd International Conference on Emerging Technologies and Factory Automation (ETFA)*, vol. 1, 2018, pp. 808–815.
- [9] P. Hu and B. Zhang, "An improved dv distance location algorithm for wireless sensor networks," in *2020 International Conference on Big Data, Artificial Intelligence and Internet of Things Engineering (ICBAIE)*, 2020, pp. 446–449.
- [10] S. Liu, Z. Wei, Z. Guo, X. Yuan, and Z. Feng, "Performance analysis of uavs assisted data collection in wireless sensor network," in *2018 IEEE 87th Vehicular Technology Conference (VTC Spring)*, 2018, pp. 1–5.
- [11] Z. Wei, Z. Feng, H. Zhou, L. Wang, and H. Wu, "Capacity and delay of unmanned aerial vehicle networks with mobility," *IEEE Internet of Things Journal*, vol. 6, no. 2, pp. 1640–1653, 2019.
- [12] N. Zhao, W. Lu, M. Sheng, Y. Chen, J. Tang, F. R. Yu, and K.-K. Wong, "Uav-assisted emergency networks in disasters," *IEEE Wireless Communications*, vol. 26, no. 1, pp. 45–51, 2019.
- [13] V. Annepu, D. R. Sona, C. V. Ravikumar, K. Bagadi, M. Alibakhshikhanari, A. A. Althwayb, B. Alali, B. S. Virdee, G. Pau, I. Dayoub, C. H. See, and F. Falcone, "Review on unmanned aerial vehicle assisted sensor node localization in wireless networks: Soft computing approaches," *IEEE Access*, vol. 10, pp. 132 875–132 894, 2022.
- [14] G. Han, J. Jiang, C. Zhang, T. Q. Duong, M. Guizani, and G. K. Karagiannidis, "A survey on mobile anchor node assisted localization in wireless sensor networks," *IEEE Communications Surveys & Tutorials*, vol. 18, no. 3, pp. 2220–2243, 2016.
- [15] L. Shen, N. Wang, Z. Zhu, Y. Fan, X. Ji, and X. Mu, "Uav-enabled data collection for mmec networks: Aem modeling and energy-efficient trajectory design," in *ICC 2020 - 2020 IEEE International Conference on Communications (ICC)*, 2020, pp. 1–6.
- [16] M. Samir, S. Sharafeddine, C. M. Assi, T. M. Nguyen, and A. Ghayeb, "Uav trajectory planning for data collection from time-constrained iot devices," *IEEE Transactions on Wireless Communications*, vol. 19, no. 1, pp. 34–46, 2020.
- [17] P. Sinha and I. Guvenc, "Impact of antenna pattern on toa based 3d uav localization using a terrestrial sensor network," *IEEE Transactions on Vehicular Technology*, vol. 71, no. 7, pp. 7703–7718, 2022.
- [18] J. Liu, P. Tong, X. Wang, B. Bai, and H. Dai, "Uav-aided data collection for information freshness in wireless sensor networks," *IEEE Transactions on Wireless Communications*, vol. 20, no. 4, pp. 2368–2382, 2021.
- [19] J. Chen and J. Tang, "Uav-assisted data collection for dynamic and heterogeneous wireless sensor networks," *IEEE Wireless Communications Letters*, vol. 11, no. 6, pp. 1288–1292, 2022.
- [20] Y. Chen, H. Liu, J. Guo, Y. Wang, F. Liu, S. Ding, and R. Chen, "Cooperative networking strategy of uav cluster for large-scale wsn," *IEEE Sensors Journal*, vol. 22, no. 22, pp. 22 276–22 290, 2022.
- [21] H. Wang, J. Wang, G. Ding, J. Chen, F. Gao, and Z. Han, "Completion time minimization with path planning for fixed-wing uav communications," *IEEE Transactions on Wireless Communications*, vol. 18, no. 7, pp. 3485–3499, 2019.
- [22] S. Yin, S. Zhao, Y. Zhao, and F. R. Yu, "Intelligent trajectory design in uav-aided communications with reinforcement learning," *IEEE Transactions on Vehicular Technology*, vol. 68, no. 8, pp. 8227–8231, 2019.
- [23] H. Sallouha, M. M. Azari, A. Chiumento, and S. Pollin, "Aerial anchors positioning for reliable rss-based outdoor localization in urban environments," *IEEE Wireless Communications Letters*, vol. 7, no. 3, pp. 376–379, 2018.
- [24] H. Sallouha, M. M. Azari, and S. Pollin, "Energy-constrained uav trajectory design for ground node localization," in *2018 IEEE Global Communications Conference (GLOBECOM)*, 2018, pp. 1–7.
- [25] X. Zou, F. Zhou, L. Fan, and W. Chen, "Shadowing cancellation and iterative newton-gradient algorithm for uav-assisted localization," *IEEE Communications Letters*, vol. 25, no. 11, pp. 3570–3574, 2021.
- [26] B. Yuan, R. He, B. Ai, R. Chen, G. Wang, J. Ding, and Z. Zhong, "A uav-assisted search and localization strategy in non-line-of-sight scenarios," *IEEE Internet of Things Journal*, vol. 9, no. 23, pp. 23 841–23 851, 2022.
- [27] Z. Wang, R. Liu, Q. Liu, J. S. Thompson, and M. Kadoch, "Energy-efficient data collection and device positioning in uav-assisted iot," *IEEE Internet of Things Journal*, vol. 7, no. 2, pp. 1122–1139, 2020.
- [28] M. Zhu, W. Xu, N. Guo, and Z. Wei, "Joint sensor localization and data collection in uav-assisted wireless sensor network," in *2022 14th International Conference on Wireless Communications and Signal Processing (WCSP)*, 2022, pp. 894–899.

- [29] Y. Zhang, B. Li, F. Gao, and Z. Han, "A robust design for ultra reliable ambient backscatter communication systems," *IEEE Internet of Things Journal*, vol. 6, no. 5, pp. 8989–8999, 2019.
- [30] S. Cao, X. Chen, X. Zhang, and X. Chen, "Combined weighted method for tdoa-based localization," *IEEE Transactions on Instrumentation and Measurement*, vol. 69, no. 5, pp. 1962–1971, 2020.
- [31] N. Okello, F. Fletcher, D. Musicki, and B. Ristic, "Comparison of recursive algorithms for emitter localisation using tdoa measurements from a pair of uavs," *IEEE Transactions on Aerospace and Electronic Systems*, vol. 47, no. 3, pp. 1723–1732, 2011.
- [32] K. K. Nguyen, T. Q. Duong, T. Do-Duy, H. Claussen, and L. Hanzo, "3d uav trajectory and data collection optimisation via deep reinforcement learning," *IEEE Transactions on Communications*, vol. 70, no. 4, pp. 2358–2371, 2022.
- [33] I. Qualcomm Technologies, "Lte unmanned aircraft systems," pp. San Diego, CA, USA, Trial report v.1.0.1, 2017.
- [34] F. Dong, L. Li, Z. Lu, Q. Pan, and W. Zheng, "Energy-efficiency for fixed-wing uav-enabled data collection and forwarding," in *2019 IEEE International Conference on Communications Workshops (ICC Workshops)*, 2019, pp. 1–6.
- [35] C. Zhan and Y. Zeng, "Completion time minimization for multi-uav-enabled data collection," *IEEE Transactions on Wireless Communications*, vol. 18, no. 10, pp. 4859–4872, 2019.
- [36] M. Hua, Y. Wang, Q. Wu, H. Dai, Y. Huang, and L. Yang, "Energy-efficient cooperative secure transmission in multi-uav-enabled wireless networks," *IEEE Transactions on Vehicular Technology*, vol. 68, no. 8, pp. 7761–7775, 2019.
- [37] J. Yang, J. Chen, and Z. Yang, "Energy-efficient uav communication with trajectory optimization," in *2021 2nd International Conference on Big Data & Artificial Intelligence & Software Engineering (ICBASE)*, 2021, pp. 508–514.
- [38] C. Wang, X. Chen, J. An, Z. Xiong, C. Xing, N. Zhao, and D. Niyato, "Covert communication assisted by uav-irs," *IEEE Transactions on Communications*, vol. 71, no. 1, pp. 357–369, 2023.
- [39] C. Zhan and R. Huang, "Energy minimization for data collection in wireless sensor networks with uav," in *2019 IEEE Global Communications Conference (GLOBECOM)*, 2019, pp. 1–6.
- [40] Y. Zeng and R. Zhang, "Energy-efficient uav communication with trajectory optimization," *IEEE Transactions on Wireless Communications*, vol. 16, no. 6, pp. 3747–3760, 2017.
- [41] Y. Zeng, J. Xu, and R. Zhang, "Rotary-wing uav enabled wireless network: Trajectory design and resource allocation," in *2018 IEEE Global Communications Conference (GLOBECOM)*, 2018, pp. 1–6.
- [42] C. Zhan and H. Lai, "Energy minimization in internet-of-things system based on rotary-wing uav," *IEEE Wireless Communications Letters*, vol. 8, no. 5, pp. 1341–1344, 2019.
- [43] M. Hua, L. Yang, Q. Wu, and A. L. Swindlehurst, "3d uav trajectory and communication design for simultaneous uplink and downlink transmission," *IEEE Transactions on Communications*, vol. 68, no. 9, pp. 5908–5923, 2020.
- [44] X. Xiong, C. Sun, W. Ni, and X. Wang, "Three-dimensional trajectory design for unmanned aerial vehicle-based secure and energy-efficient data collection," *IEEE Transactions on Vehicular Technology*, vol. 72, no. 1, pp. 664–678, 2023.
- [45] H. Huang and A. V. Savkin, "Path planning for a solar-powered uav inspecting mountain sites for safety and rescue," *Energies*, vol. 14, no. 7, p. 1968, 2021.
- [46] C. Zhan and R. Huang, "Energy minimization for data collection in wireless sensor networks with uav," 2019.
- [47] Y. Shi and R. Eberhart, "Empirical study of particle swarm optimization," in *Proceedings of the 1999 Congress on Evolutionary Computation-CEC99 (Cat. No. 99TH8406)*, vol. 3, 1999, pp. 1945–1950 Vol. 3.